

Dynamics of locomotion in the seed harvesting ant *Messor barbarus*: Effect of individual body mass and transported load mass

Hugo Merienne¹, Gérard Latil¹, Pierre Moretto¹, Vincent Fourcassié^{Corresp. 1}

¹ Centre de Recherches sur la Cognition Animale, Centre de Biologie Intégrative, Université de Toulouse, CNRS, UPS, Toulouse, France

Corresponding Author: Vincent Fourcassié

Email address: vincent.fourcassie@univ-tlse3.fr

Ants are well-known for their amazing load carriage performances. Yet, the biomechanics of locomotion during load transport in these insects has so far been poorly investigated. Here, we present a study of the biomechanics of unloaded and loaded locomotion in the polymorphic seed-harvesting ant *Messor barbarus* (Linnaeus, 1767). This species is characterized by a strong intra-colonial size polymorphism with allometric relationships between the different body parts of the workers. In particular, big ants have much larger heads relative to their size than small ants. Their center of mass is thus shifted forward and even more so when they are carrying a load in their mandibles. We investigated the dynamics of the ant center of mass during unloaded and loaded locomotion. We found that during both unloaded and loaded locomotion, the kinetic energy and gravitational potential energy of the ant center of mass are in phase, which is in agreement with what has been described by other authors as a grounded-running gait. During unloaded locomotion, small and big ants do not display the same posture. However, they expend the same amount of mechanical energy to raise and accelerate their center of mass per unit of distance and per unit of body mass. While carrying a load, compared to the unloaded situation, ants seem to modify their locomotion gradually with increasing load mass. Therefore, loaded and unloaded locomotion do not involve discrete types of gait. Moreover, small ants carrying small loads expend less mechanical energy per unit of distance and per unit of body mass and their locomotion thus seem more mechanically efficient.

1 **Dynamics of locomotion in the seed harvesting ant**
2 ***Messor barbarus*: effect of individual body mass and**
3 **transported load mass**

4

5 Hugo Merienne¹, Gérard Latil¹, Pierre Moretto¹, Vincent Fourcassié¹

6

7 ¹ Centre de Recherches sur la Cognition Animale, Centre de Biologie Intégrative, Université de
8 Toulouse, CNRS, UPS, France.

9

10 Corresponding Author:

11 Vincent Fourcassié

12 Email address : vincent.fourcassie@univ-tlse3.fr

13

14 Street address : Centre de Recherches sur la Cognition Animale (UMR 5169) - Centre de
15 Biologie Intégrative - CNRS - Université Paul Sabatier - Bât 4R3, 710, cours Rosalind Franklin.
16 118, route de Narbonne. 31062 Toulouse cedex 09 - France

17 **Abstract**

18 Ants are well-known for their amazing load carriage performances. Yet, the biomechanics of
19 locomotion during load transport in these insects has so far been poorly investigated. Here, we
20 present a study of the biomechanics of unloaded and loaded locomotion in the polymorphic seed-
21 harvesting ant *Messor barbarus* (Linnaeus, 1767). This species is characterized by a strong intra-
22 colonial size polymorphism with allometric relationships between the different body parts of the
23 workers. In particular, big ants have much larger heads relative to their size than small ants.
24 Their center of mass is thus shifted forward and even more so when they are carrying a load in
25 their mandibles. We investigated the dynamics of the ant center of mass during unloaded and
26 loaded locomotion. We found that during both unloaded and loaded locomotion, the kinetic
27 energy and gravitational potential energy of the ant center of mass are in phase, which is in
28 agreement with what has been described by other authors as a grounded-running gait. During
29 unloaded locomotion, small and big ants do not display the same posture. However, they expend
30 the same amount of mechanical energy to raise and accelerate their center of mass per unit of
31 distance and per unit of body mass. While carrying a load, compared to the unloaded situation,
32 ants seem to modify their locomotion gradually with increasing load mass. Therefore, loaded and
33 unloaded locomotion do not involve discrete types of gait. Moreover, small ants carrying small
34 loads expend less mechanical energy per unit of distance and per unit of body mass and their
35 locomotion thus seems more mechanically efficient.

36

37 **Introduction**

38 Locomotion is a crucial aspect of animal behavior. It is essential to accomplish tasks such as
39 searching for food or a shelter, hunting for prey, looking for a mate or escaping a predator. For
40 each of these tasks, animals have to adjust specific features of their locomotion in order to
41 behave optimally (Halsey, 2016). Different ways of moving are thus used by animals, each most
42 fitted to a given situation. Among walking animals, insects are of particular interest for the study
43 of locomotion due to their outstanding performances, as attested by the maximum speed some
44 insects can reach, e.g. about 40 body lengths per second for the ant *Cataglyphis bombycina*
45 (Pfeffer *et al.*, 2019) or about 35 body lengths per second for the cockroach *Periplaneta*
46 *americana* (Full and Tu, 1991). This probably explains why insects have been for decades a

47 source of inspiration for the design of legged robots (Kar *et al.*, 2003; Koditschek *et al.*, 2004;
48 Dupeyroux *et al.*, 2019).

49 From a purely kinematic point of view, the most common locomotory gait encountered in insects
50 is the alternating tripod gait (Delcomyn, 1981), in which the swing phase of a set of three legs
51 called tripods (the ipsilateral front and hind leg and the contralateral mid leg) is synchronized
52 with the contact phase of the contralateral tripod. However, this pattern can be altered by many
53 factors. For example, it can vary with the speed (Bender *et al.*, 2011; Wosnitza *et al.*, 2012;
54 Mendes *et al.*, 2013; Wahl *et al.*, 2015), the behavior (exploration: Reinhardt *et al.*, 2009;
55 Reinhardt and Blickhan, 2014; wall-following: Bender *et al.*, 2011; backward locomotion:
56 Pfeffer *et al.*, 2016), the external (leg amputation: Fleming and Bateman, 2007; Gruhn *et al.*,
57 2009; Grabowska *et al.*, 2012) and internal state (effects of ageing: Ridgel and Ritzmann, 2005;
58 blocking of proprioceptive feedback: Mendes *et al.*, 2013) of the insects, as well as with the
59 characteristics of their physical environment, such as the type of substrate on which they walk
60 (Spence *et al.*, 2010), the presence of wind (Full and Koehl, 1993), the slope of the terrain
61 (Diederich, 2006; Seidl and Wehner, 2008; Moll *et al.*, 2010; Grabowska *et al.*, 2012; Wöhrle *et al.*
62 *et al.*, 2017), and the presence of obstacles (Watson *et al.*, 2002).

63 One of the factors that is known to affect locomotory gait in humans (Ahmad and Barbosa, 2019)
64 and other vertebrates (review by Jagnandan and Higham, 2018), but that has so far received little
65 attention in insects, is load carriage. Load carriage occurs in insects mostly internally, for
66 example after ingesting food or when a female insect carry eggs. However, these internal loads
67 only induce small changes in the total mass of individuals. Much more impressive are the
68 external loads that are carried by some insects while returning to their nest. In ants in particular,
69 these loads can be considerable and weigh more than ten times the body mass of individuals
70 (Bernadou *et al.*, 2016). They can shift the Center of Mass (CoM) of individuals forward and
71 thus have a strong impact on their locomotion. The changes induced by load carriage on the
72 locomotion of ants have so far been investigated only with a kinematic approach, through the
73 analysis of stepping pattern (Zollikofer, 1994; Moll *et al.*, 2013; Merienne *et al.*, 2020). In the
74 seed harvesting ant *Messor barbarus* for example, load carriage has been found to decrease
75 locomotory speed (through a decrease in stride frequency but not of step amplitude), to increase
76 the mean number of legs in contact with the ground, as well as to induce a change in leg
77 positioning, with ants spreading their legs further away from their longitudinal body axis in order

78 to maintain their stability (Merienne *et al.*, 2020). On the other hand, the impact of load carriage
79 on the exchanges of mechanical energies and on the mechanical cost of locomotion in ants is
80 poorly documented. Here, we aim to fill this gap by investigating the impact of load carriage on
81 the CoM dynamics in individuals of the species *M. barbarus* (Linnaeus, 1767) whose workers
82 routinely transport items weighing up to thirteen times their own mass over dozen of meters
83 (Bernadou *et al.*, 2016). Individuals of this species show a high variation in size within colonies,
84 with a body mass ranging from 1.7 to 40.0 mg. This variation is continuous and is characterized
85 by a positive allometry between head size and thorax length (Heredia & Detrain, 2000; Bernadou
86 *et al.*, 2016), which means that, relative to their size, the head of large workers is bigger than that
87 of small workers. Consequently, the CoM of big workers is shifted forward compared to that of
88 small workers (Bernadou *et al.*, 2016; see also Anderson *et al.*, 2020 for ants of the genus
89 *Pheidole*). In our study we thus chose to investigate both the effect of body mass and load mass
90 on the locomotion of loaded ants. We varied in a systematic way the mass of the load carried by
91 ants of different sizes so as to cover the same range of load ratio. We then compared the
92 displacement of the CoM and its mechanical work, which represents the amount of mechanical
93 energy needed to raise the CoM and accelerate it during locomotion, of the same individuals in
94 unloaded and loaded condition. Since external load carriage is already observed in wasps
95 (Polidori *et al.*, 2013), which are considered as the ant ancestors (Peters *et al.*, 2017), we
96 hypothesized that ants could have evolved some mechanisms to transport loads economically.
97 Specifically, we tested the assumption that, ants, in the same way as humans (Heglund *et al.*,
98 1995), could be able to decrease, or at least compensate, the additional mechanical cost of
99 carrying a load by improving the pendulum-like behavior of their CoM through a better transfer
100 between the gravitational potential and kinetic energy of their CoM. Moreover, since large ants
101 have a less stable locomotion than small ants (Merienne *et al.*, 2020) due to the forward shift of
102 their CoM, we predict that their locomotion when transporting loads representing the same
103 amount of individual body mass should be less mechanically efficient than that of small ants, and
104 the more so for loads of increasing mass.

105

106 **Material and methods**

107 Note that the data presented in this paper are part of the data collected in the study presented in
108 Merienne *et al.* (2020). The studied species, experimental setup and experimental protocol are
109 thus the same.

110 **Studied species**

111 Experiments were carried out with a large colony of *M. barbarus* collected in April 2018 at St
112 Hippolyte (Pyrénées Orientales), on the French Mediterranean coast. Workers in the colony
113 ranged from 2 to 15 mm in length and from 1 to 40 mg in body mass. The colony was housed in
114 glass tubes with a water reservoir at one end and kept in a room at 26°C with a 12:12 L:D
115 regime. The tubes were placed in a box (LxWxH: 0.50x0.30x0.15 m) whose walls were coated
116 with Fluon® to prevent ants from escaping. During the experimental period, ants were fed with a
117 mixture of seeds of various species and had access *ad libitum* to water.

118 **Experimental setup**

119 Ants were tested on a setup designed and built by a private company (R&D Vision, France,
120 <http://www.rd-vision.com>). It consisted in a walking platform surrounded by five high speed
121 cameras (JAI GO-5000M-PMCL: frequency: 250Hz; resolution: 30µm/px for the top camera,
122 20µm/px for the others). One camera was placed above the platform and four were placed on its
123 sides. The platform was 160mm long and 25mm wide and was covered with a piece of black
124 paper (Canson®, 160g/m²). Four infrared spots ($\lambda=850\text{nm}$, pulse frequency= 250 Hz)
125 synchronized with the cameras illuminated the scene from above. The mean temperature in the
126 middle of the platform, measured with an infrared thermometer (MS pro, Optris, USA,
127 <http://www.optris.com>) over the course of the experiment, was (mean \pm SD) 28 ± 1.4 °C.

128 **Experimental protocol**

129 We performed all experiments between April and July 2018.

130 We wanted to make sure that the ants we tested were foraging workers. Therefore, the first day
131 of an experimental session, we selected a random sample of workers returning to their nest with
132 a seed on a foraging trail established between the box containing the colony and a seed patch.

133 We then kept these ants in a separate box and used them in our experiments the following days.

134 Each ant was tested twice: the first time unloaded and the second time loaded with a fishing lead
135 glued on its mandibles. Before being tested, unloaded ants were first weighed to the nearest 0.1
136 mg with a precision balance (NewClassic MS semi-micro, Mettler Toledo, United States).

137 Individual ants were then gently placed at one end of the platform and we started recording their
138 locomotion as soon as they entered the camera fields. The recording was retained only if ants
139 walked straight for at least three full strides, a stride being defined as the interval of time elapsed
140 between two consecutive lift off of the right mid leg. All videos were subsequently cropped to a
141 whole number of strides. To stimulate the ants and to obtain a straighter path, an artificial
142 pheromone trail was laid down along the middle axis of the platform by depositing every
143 centimeter a small drop of a hexane solution of Dufour gland (1 gland / 20 μ l), which is
144 responsible for the production of trail pheromone in *M. barbarus* (Heredia and Detrain, 2000).
145 This operation was renewed every 45 minutes in order to keep a fresh trail on the platform.

146 Once five ants were tested in unloaded condition, we proceeded with the test in loaded condition.
147 First, each ant was anesthetized by putting it in a vial plunged in crushed ice. It was then fixed on
148 its back, with its head maintained horizontally, and we glued a calibrated fishing lead on its
149 mandibles with a droplet of superglue (Loctite, <http://www.loctite.fr>). After letting the glue dry
150 for 15 minutes and the ant recover for half an hour, the ant was placed again on the platform and
151 its locomotion was recorded in loaded condition. We retained only the recordings in which the
152 load did not touch the ground during the transport (see Merienne *et al.*, 2020). At the end of the
153 recording, the ant was captured and weighed a second time. It was then killed and each of its
154 body parts (head, thorax, gaster) was weighed separately.

155 **Data extraction and analysis**

156 In order to compute the 3D displacement of the ants' main body parts (head, thorax, gaster) and
157 of its overall CoM, we tracked several anatomic points on the view of the top camera (Fig. 1A-
158 C) and on the view of one of the side cameras (Fig. 1B-D) with the software Kinovea (version
159 0.8.15, <https://www.kinovea.org>).

160 We assumed a homogeneous distribution of the mass within each body parts and thus computed
161 the (X, Y) coordinates of the CoM of the three main body parts (plus the load) as the mean of the
162 (X, Y) coordinates of the two points tracked at their extremities on the top view and the vertical
163 position (Z) as the mean of the vertical position of the two points tracked on each of these parts
164 on the side view. For each frame we computed the position of the overall CoM of an ant as the
165 barycenter of the CoM of its three main body parts (plus the load for loaded ants) weighted by
166 their mass. For each ant tested, we delimited the different strides on the videos and then, for each

167 stride, we calculated the positions (X, Y, Z) and velocity vectors of the overall CoM. Finally, we
168 averaged the CoM speeds and positions across the multiple stride cycles in order to obtain a
169 single mean trajectory of the CoM in each condition (unloaded and loaded).

170 In order to characterize the mean trajectories of the CoM for each ant and condition, we
171 computed the peak-to-peak amplitude of the Z positions of the CoM and assessed the sinus-like
172 behavior of the changes in Z position and in the norm of the velocity vector. In order to do so, we
173 first normalized the Z positions and the values of the norm of the velocity vector by their
174 respective peak-to-peak amplitude and fitted a sinus function to the resulting signals. We then
175 computed the root-mean-square error (RMSE) between the fitted function and the normalized
176 data.

177 In order to assess the general posture of the ants during locomotion, we also computed the mean
178 Z position of their CoM in units of body length and the mean inclination angle of their body
179 during locomotion (defined as the angle between the horizontal X axis and the line linking the
180 gaster and head CoMs).

181 From the dynamic of the CoM, we then computed its kinetic E_k and gravitational potential E_p
182 energies relative to the surroundings with the formulae

$$183 \quad E_k = 0.5 * m * v^2 \quad (1)$$

184 and

$$185 \quad E_p = m * g * h \quad (2)$$

186 where m is the mass of the ant (plus the mass of the load if one is carried), v the speed of the
187 CoM, g the gravitational constant and h the vertical position of the CoM above the walking
188 platform. We then computed the external mechanical energy of the CoM as the sum of the
189 kinetic and potential energies.

190 Finally, following Bastien *et al.* (2016), we computed the external mechanical work (W_{ext})
191 achieved to raise and accelerate the CoM as the sum of the positive increments of the external
192 mechanical energy. Since ants did not walk the same distance or during the same amount of time,
193 in order to compare the mechanical work they achieved, we divided W_{ext} by the distance
194 travelled and thus obtained a “mechanical work per unit distance” $W_{ext,d}$. This makes sense if

195 one considers that locomotion is a repetitive process and that we cropped our videos to a whole
 196 number of strides. We then computed the mean external power (P_{ext}) by dividing W_{ext} by the
 197 duration of locomotion. Finally, we computed the mass specific values of $W_{ext,d}$ and P_{ext} by
 198 dividing both of these metrics by the ant mass for unloaded locomotion and the ant mass plus
 199 load mass for loaded locomotion.

200 Following Cavagna *et al.* (1976) we then computed the energy recovered (R , expressed in
 201 percentage) through the pendulum-like oscillations of the CoM with the formula :

$$202 \quad R = 100 * \frac{W_k + W_p - W_{ext}}{W_k + W_p} \quad (3)$$

203 Where W_k is the sum of the positive increments of the kinetic energy versus time curve and W_p
 204 is the sum of the positive increments of the potential energy versus time curve. R is an indicator
 205 of the amount of energy transferred between the potential and the kinetic energy of the CoM due
 206 to its pendulum-like behavior: the closer the value of R to 100%, the more consistent the
 207 locomotor pattern is with the Inverted Pendulum System (IPS) model (Cavagna *et al.*, 1977) in
 208 which the fluctuations of E_p and E_k are perfectly out of phase, i.e., all the kinetic energy of the
 209 CoM is transformed in potential energy, and vice versa, over a stride.

210 In order to further characterize the relationship between E_k and E_p , we computed the Pearson
 211 correlation coefficient between E_k and E_p , and, following Ahn *et al.* (2004) and Vereecke *et al.*
 212 (2006), the percentage congruity between E_k and E_p (defined as the percentage of time E_k and
 213 E_p changed in the same direction). We then fitted a sinus function to the variations of both E_k
 214 and E_p , extracted the phase of E_k and E_p from these sinus functions, and computed the difference
 215 between the two phases in order to access the phase lag between E_k and E_p (a positive value of
 216 this lag indicating that E_k is late compared to E_p).

217 For the unloaded condition, we expressed all variables Y as a power law function of ant mass M ,
 218 i.e., $Y = a * M^b$ (Merienne *et al.*, 2020). For each variable, the values of the coefficients a and b ,
 219 as well as the value of the variable predicted by the statistical model for the mean mass of the
 220 tested ants (12.5 mg), are given in a table, along with their 95% confidence interval. For the
 221 loaded condition, we computed for each ant the ratio of the value of each variable between the
 222 loaded Y_l and unloaded Y_u condition. This ratio was then expressed as a power law function of

223 both ant mass M and load ratio LR , defined as $1 + (\text{load mass}/\text{ant body mass})$ (Bartholomew *et*
224 *al.*, 1988), i.e., $\frac{Y_l}{Y_u} = c * M^d * LR^e$ (Merienne *et al.*, 2020). The value of the coefficients c , d for
225 ant mass, e for load ratio for each variable, as well as the value of the variable predicted by the
226 statistical model for the mean mass of tested ants and a load ratio of one, along with their 95%
227 confidence interval, are given in a table. The coefficients d and e are positive when the response
228 variable increases with increasing value of ant mass and load ratio, they are negative in the other
229 case.

230 All data analyses were performed and graphics designed with R (v. 3.5.1) run under RStudio (v.
231 1.0.136). The *confint()* function was used to calculate the confidence intervals of the model
232 coefficients.

233

234 **Results**

235 In total, 52 ants whose body mass ranged from 1.7 to 33.0 mg were tested in both unloaded and
236 loaded conditions, with a load ratio ranging from 1.2 to 7.0 (Fig. 2).

237 **Unloaded ants: influence of body mass**

238 The analysis of the position of the CoM shows that there was no evidence of a periodic pattern
239 on the Y axis. On the Z axis on the other hand, the position of the CoM (Fig. 3A), as well as its
240 speed norm (Fig. 3B), followed a periodic pattern that was well approximated by a sinus
241 function, as shown by the low value of the RMSE (Table 1, line 1 & 2). Interestingly, the
242 amplitude of the oscillations of the CoM Z position seems to be approximately the same for
243 small and big ants (Fig. 3A). Indeed, the relative amplitude (expressed in units of body length,
244 Table 1, line 3) of the oscillations of the CoM Z position, as well as its mean relative position
245 (Table 1, line 4), decreased significantly with increasing ant mass ($F_{1,52} = 75.88$, $P < 0.001$ and
246 $F_{1,52} = 105.24$, $P < 0.001$, respectively). The CoM of big ants was thus relatively lower and
247 oscillated with a relatively smaller amplitude than that of small ants. The ant body angle was
248 independent of ant mass (Table 1, line 5).

249 The variations of E_k and E_p were periodic and the amplitude of E_p was much greater than that of
250 E_k in both small (Fig. 4A) and big ants (Fig. 4B). E_k and E_p were mostly in phase, as shown by
251 the high values of both the correlation coefficient (Table 1, line 6) and the percentage congruity

252 (Table 1, line 7). Nevertheless, E_k and E_p were more in phase for small ants than for big ants (Fig.
253 5A). The phase lag between the variation of potential and kinetic energies was positive (Fig. 5B)
254 and increased with increasing ant mass (Table 1, line 8: $F_{1,52} = 11.51$, $P=0.001$). As a
255 consequence, E_k and E_p were more out of phase for big ants compared to small ants and thus both
256 the correlation coefficient (Table 1, line 6) and the percentage congruity (Table 1, line 7)
257 decreased with increasing ant mass ($F_{1,52} = 5.79$, $P=0.020$ and $F_{1,52} = 4.75$, $P=0.034$,
258 respectively).

259 The external mechanical work of the CoM per unit distance ($W_{ext,d}$) increased with increasing ant
260 mass (Fig. 6A). However, there was no relationship between the mass-specific external
261 mechanical work of the CoM per unit distance ($W_{ext,d}/m$) and ant mass (m) (Table 1, line 9). In
262 the same way, the mean external mechanical power of the CoM (P_{ext}) increased with increasing
263 ant mass (Fig. 6B) but there was no relationship between the mass-specific external mechanical
264 power of the CoM (P_{ext}/m) and ant mass (Table 1, line 10).

265 The percentage of energy recovery was very low and did not depend on ant mass (Table 1, line
266 11).

267 **Loaded ants: influence of ant mass and load ratio**

268 In the same way as in unloaded condition, no periodicity was found in the CoM Y trajectory in
269 the loaded condition. On the Z axis, independent of ant mass, the sinus-like periodicity of the Z
270 position of the CoM (assessed by the Z position RMSE) decreased with increasing load ratio
271 (Fig. 3C and 3E, Table 2, line 2: $F_{1,52}=3.87$, $P=0.010$). We found no significant changes in the
272 relative amplitude of the oscillations of the CoM Z position (Table 2, line 3) and in the mean Z
273 position of the CoM (Table 2, line 4) between the unloaded and loaded condition, whatever the
274 ant mass and load ratio. The speed of the CoM in loaded condition followed a periodic pattern
275 (Fig. 3D and 3F) that was well approximated by a sinus function, whatever the values of ant
276 mass and load ratio (Table 2, line 1). Independent of ant mass and load ratio, the ant body angle
277 did not change between the unloaded and loaded condition (Table 2, line 5).

278 In the same way as in unloaded condition, E_k and E_p were mostly in phase for low load ratio in
279 small (Fig. 4C) and big ants (Fig. 4D), but less so for high load ratio (Fig. 4E and 4F).

280 Independent of ant mass and load ratio, the correlation coefficient between E_k and E_p did not
281 vary significantly between the unloaded and loaded condition (Fig. 5A, Table 2, line 6) and the

282 phase lag only slightly decreased (Fig. 5B, Table 2, line 8). However, independent of ant mass,
283 the percentage congruity decreased for ants carrying loads of increasing load ratio (Table 2, line
284 7: $F_{1,52} = 8.22$, $P < 0.001$). In the loaded condition, in the same way as in the unloaded condition,
285 E_k and E_p were more in phase for small ants than for big ants (Fig. 5A). However, contrary to the
286 unloaded condition, the phase lag was not statistically different between small and big ants in the
287 loaded condition (Fig. 5B).

288 Independent of load ratio, the mass-specific $W_{ext,d}$ increased with increasing ant mass (Table 2,
289 line 9: $F_{2,51} = 12.47$, $P = 0.024$) and, independent of ant mass, it also increased with increasing
290 load ratio ($F_{2,51} = 12.47$, $P < 0.001$). However, there was no effect of the load on the mass-specific
291 P_{ext} (Table 2, line 10). Finally, there was no significant change in percentage recovery between
292 the unloaded and loaded condition (Table 2, line 11).

293

294 Discussion

295 In this study, we investigated the dynamics of locomotion of unloaded and loaded individuals of
296 the polymorphic ant *M. barbarus*. We found that during unloaded locomotion the variations of
297 the speed of the CoM and of its vertical position are characterized by a periodic pattern, with two
298 periods corresponding to the two steps included in one stride. These variations were well
299 described by a sinus function, although the pattern of variation of the CoM Z position was
300 strongly affected by load transport. The kinetic and potential energies were mostly in phase
301 during unloaded locomotion, which led to very low energy recovery values. With increasing load
302 however, the variations in potential energy became much greater than the variations in kinetic
303 energy. Therefore, ants achieved mechanical work mainly to raise their CoM rather than to
304 accelerate it. The external mechanical work ants had to perform to raise and accelerate their CoM
305 over a locomotory cycle did not vary with body mass for unloaded ants and increased with load
306 ratio for ants of same body mass.

307 Unloaded ants

308 During unloaded locomotion, the mean of the absolute Z position of the CoM, as well as the
309 amplitude of its variations, did not differ between small and big ants. Therefore, relative to their
310 size, the body of small ants was higher over the ground than that of big ants and their CoM made
311 greater vertical oscillations. This difference cannot be explained by a change in body inclination

312 because this latter did not change between small and big ants. It thus seems that small ants are
313 walking in a more erect posture than big ants. This could be related to a more excited state of
314 small ants compared to big ants in response to manipulation, as also suggested by their higher
315 locomotory speed relative to their size (Merienne *et al.* 2020). Such a difference between ants of
316 different sizes in response to threat has already been found in other ant species, e.g. the leaf-
317 cutting ant *Atta capiguara* (Hughes and Goulson, 2001), and this could be related to the division
318 of labor within colonies. Further experiments should be performed to answer this question.

319 The kinetic and potential energies of the CoM were mainly in phase during unloaded
320 locomotion, which led to very low energy recovery values (7-9 %). These values are similar to
321 those reported by Full and Tu (1991) in the cockroach *Periplaneta americana* and a bit below
322 those reported in the cockroach *Blaberus discoidalis* (Full and Tu, 1990) and in the ant *Formica*
323 *polyctena* (Reinhardt and Blickhan, 2014). These values are not consistent with the inverted
324 pendulum model of Cavagna *et al.* (1977). As walking ants never display aerial phases
325 (Merienne *et al.* 2020), their locomotion is thus rather better characterized as a form of *grounded*
326 *running* (*Formica polyctena* : Reinhardt and Blickhan 2014).

327 No differences were observed in the mass specific external mechanical work nor in the mass
328 specific external mechanical power between individuals of different sizes. This is in agreement
329 with the literature, which shows that the mass specific external mechanical work is constant over
330 a wide range of animal species ranging from 10g to 100kg in body mass (Full & Tu, 1991;
331 Alexander, 2005). The value we found in *M. barbarus* workers (mean \pm SD: $1.082 \pm 0.175 \text{ J.m}^{-1}$
332 $\cdot \text{kg}^{-1}$) is very close to that reported in the literature for a wide variety of organisms, i.e. just
333 above $1 \text{ J.m}^{-1} \cdot \text{kg}^{-1}$.

334 **Loaded ants**

335 Independent of ant mass, we did not observe any changes in the mean CoM Z position and in the
336 amplitude of the oscillations of the CoM Z position in loaded ants. Even if the CoM mean speed
337 decreased in loaded ants (Merienne *et al.*, 2020), this decrease seems to have little impact on the
338 sinus-like variation of the CoM speed (Fig. 3D and 3F). On the other hand, the pattern of
339 variation of the CoM Z position was strongly affected by heavy loads. The locomotion was much
340 more jerky and the variations in the CoM Z position could not be approximated by a sinus
341 function, especially for big ants (Fig. 3E). Moreover, because of the decrease in locomotory

342 speed due to carrying a load (Merienne *et al.*, 2020) and the amplitude of the CoM Z position
343 which remained unchanged, the amplitude of the variation of the CoM potential energy became
344 much greater than that of the kinetic energy (Fig. 4C-F). The mechanical energy required to raise
345 the CoM in loaded ants is thus much greater than that required to accelerate it in the forward
346 direction. Therefore, the variations in the CoM potential energy and in the CoM mechanical
347 energy are nearly identical and the external mechanical work is mostly achieved for raising the
348 CoM.

349 Independent of ant mass, the mass specific mechanical work increased with load ratio. This is an
350 unexpected result as the mass specific mechanical work is independent of load ratio in humans
351 (Bastien *et al.*, 2016). It is thus mechanically more costly for ants to move one unit of mass on
352 one unit of distance during loaded locomotion than during unloaded locomotion. Moreover,
353 independent of load ratio, the mass specific mechanical work increased with ant mass, which
354 means that the mechanical work big ants have to perform in order to raise one unit mass of their
355 body on one unit of distance is greater than that of small ants.

356 Compared to unloaded locomotion, none of the gait parameters we studied was modified in a
357 discrete way in loaded locomotion. We conclude that ants do not use a specific gait in order to
358 carry a load. Rather, they adapt their locomotion to the mass of the load they transport.

359 In this study we focused only on the external mechanical work ants have to perform in order to
360 raise and accelerate their CoM. Therefore, we did not take into account the movement of the leg
361 segments in the determination of both the position of the overall CoM and the internal
362 mechanical work that ants have to perform in order to accelerate their legs relative to their CoM.
363 Kram *et al.* (1997) found in the cockroach *Blaberus discoidalis* that this internal work represents
364 about 13% of the external mechanical work generated to lift and accelerate the CoM.

365 Considering that the stride frequency of *M. barbarus* (mean \pm SD: 4.8 ± 0.9 Hz, Merienne *et al.*,
366 2020) is lower than that of *B. discoidalis* (mean \pm SD: 6.8 ± 0.8 Hz, Kram *et al.*, 1997), if one
367 assumes that the mass of the legs of *M. barbarus* workers represents the same percentage of total
368 body mass as that of *B. discoidalis*, i.e. 10-12% (Kram *et al.*, 1997), we would expect the internal
369 mechanical work to represent a smaller part of the total mechanical work in *M. barbarus*
370 compared to *B. discoidalis*. Despite the technical difficulties for tracking the 3D displacement of

371 insect legs (but see: Uhlmann *et al.* 2017), this aspect could constitute an interesting perspective
372 for further studies.

373

374 **Conclusion**

375 Unloaded ants adopted different postures according to their size. Small ants were more erected
376 on their legs than big ants and their CoM showed greater vertical oscillations. However, this did
377 not affect the amount of energy per unit of distance and unit of body mass required to raise and
378 accelerate their CoM. Both for unloaded and loaded locomotion, the kinetic and potential
379 energies were mainly in phase, which corresponds to the grounded-running gait described by
380 Reinhardt and Blickhan (2014) during unloaded locomotion in the ant *Formica polyctena*.

381 Regarding loaded locomotion, the amount of energy needed to raise and accelerate the center of
382 mass per unit of distance and unit of body mass increased with increasing body mass and load
383 mass, suggesting that, in this respect, smaller ants carrying smaller loads were mechanically
384 more efficient during locomotion. This could be related to the division of labor observed on the
385 foraging trails of *M. barbarus*. In fact, relative to the proportion they represent on foraging trails,
386 workers of intermediate size, i.e. *media*, contribute the largest share of seed transport, compared
387 to small or big workers. Big workers are mostly present at the end of the trails where they climb
388 on the plants to cut thick stalks or spikelets, or inside the nest, to mill the seeds and prepare them
389 for consumption.

390

391 **Acknowledgements**

392 The authors wish to thank Ewen Powie and Loreen Rupprecht for their help in video analysis and
393 data extraction. Thanks are also due to Melanie Debelgarric for designing the Dufour gland
394 extraction protocol.

395

396 **References**

- 397 Ahmad HN, Barbosa TM. 2019. The effects of backpack carriage on gait kinematics and kinetics
398 of schoolchildren. *Scientific Reports* 9:1–6. doi:10.1038/s41598-019-40076-w
- 399 Ahn AN, Furrow E, Biewener AA. 2004. Walking and running in the red-legged running frog,
400 *Kassina maculata*. *Journal of Experimental Biology* 207:399–410. doi: 10.1242/jeb.00761
- 401 Alexander RM. 2005. Models and the scaling of energy costs for locomotion. *Journal of*
402 *experimental biology* 208:1645–1652. doi:10.1242/jeb.01484
- 403 Anderson PSL, Rivera MD, Suarez AW. 2020. "Simple" biomechanical model for ants reveals
404 how correlated evolution among body segments minimizes variation in center of mass as
405 heads get larger. *Integrative and Comparative Biology*, 1–15. doi:10.1093/icb/icaa027
- 406 Bartholomew GA, Lighton JRB, Feener DH Jr. 1988. Energetics of trail running, load carriage,
407 and emigration in the column-raiding army ant *Eciton hamatum*. *Physiological Zoology*, 61:
408 57-68.
- 409 Bastien GJ, Willems PA, Schepens B, Heglund NC. 2016. The mechanics of head-supported
410 load carriage by Nepalese porters. *Journal of Experimental Biology* 219:3626–3634. doi:
411 10.1242/jeb.143875
- 412 Bender JA, Simpson EM, Tietz BR, Daltorio KA, Quinn RD, Ritzmann RE. 2011. Kinematic
413 and behavioral evidence for a distinction between trotting and ambling gaits in the
414 cockroach *Blaberus discoidalis*. *Journal of Experimental Biology* 214:2057–2064.
415 doi:10.1242/jeb.056481
- 416 Bernadou A, Felden A, Moreau M, Moretto P, Fourcassié V. 2016. Ergonomics of load transport
417 in the seed harvesting ant *Messor barbarus* : morphology influences transportation method
418 and efficiency. *Journal of Experimental Biology* 219:2920–2927. doi:10.1242/jeb.141556
- 419 Cavagna GA, Heglund NC, Taylor CR. 1977. Mechanical work basic mechanisms in terrestrial
420 locomotion : two for minimizing energy expenditure. *American Journal of Physiology*
421 233:243–261. doi:10.1152/ajpregu.1977.233.5.R243
- 422 Cavagna GA, Thys H, Zamboni A. 1976. The source of external work in level walking and
423 running. *Journal of Physiology* 262:639–657. doi:10.1113/jphysiol.1976.sp011613

- 424 Delcomyn F. 1981. *Locomotion and Energetics in Arthropods*. Springer US.
- 425 Diederich B. 2006. Stick insects walking along inclined surfaces. *Integrative and Comparative*
426 *Biology* 42:165–173. doi: 10.1093/icb/42.1.165
- 427 Dupeyroux J, Serres JR, Viollet S. 2019. AntBot: A six-legged walking robot able to home like
428 desert ants in outdoor environments. *Science Robotics* 4:1–13. doi:
429 10.1126/scirobotics.aau0307
- 430 Fleming PA, Bateman PW. 2007. Just drop it and run: the effect of limb autotomy on running
431 distance and locomotion energetics of field crickets (*Gryllus bimaculatus*). *Journal of*
432 *Experimental Biology* 210:1446–1454. doi:10.1242/jeb.02757
- 433 Full RJ, Koehl MR. 1993. Drag and lift on running insects. *Journal of Experimental Biology*
434 176:89–101.
- 435 Full RJ, Tu MS. 1990. Mechanics of six-legged runners. *Journal of experimental biology*
436 148:129–146.
- 437 Full RJ, Tu MS. 1991. Mechanics of a rapid running insect: two-, four- and six-legged
438 locomotion. *Journal of Experimental Biology* 231:215–231.
- 439 Grabowska M, Godlewska E, Schmidt J, Daun-Gruhn S. 2012. Quadrupedal gaits in hexapod
440 animals - inter-leg coordination in free-walking adult stick insects. *Journal of Experimental*
441 *Biology* 215:4255–4266. doi: 10.1242/jeb.073643
- 442 Gruhn M, Zehl L, Büschges A. 2009. Straight walking and turning on a slippery surface. *Journal*
443 *of Experimental Biology*, 212: 194-209. doi:10.1242/jeb.018317
- 444 Halsey LG. 2016. Terrestrial movement energetics: current knowledge and its application to the
445 optimising animal. *Journal of Experimental Biology* 219:1424–1431.
446 doi:10.1242/jeb.133256
- 447 Heglund NC, Willems PA, Penta M, Cavagna GA. 1995. Energy-saving gait mechanics with
448 head-supported loads. *Nature* 375:52–53. doi: 10.1038/375052a0.
- 449 Heredia A, Detrain C. 2000. Worker size polymorphism and ethological role of sting associated
450 glands in the harvester ant *Messor barbarus*. *Insectes Sociaux* 47:383–389.
- 451 Hughes WOH, Goulson D. 2001. Polyethism and the importance of context in the alarm reaction

- 452 of the grass-cutting ant, *Atta capiguara*. *Behavioral Ecology and Sociobiology* 49:503–508.
453 doi: 10.1007/s002650100321
- 454 Jagnandan K, Higham TE. 2018. How rapid changes in body mass affect the locomotion of
455 terrestrial vertebrates: Ecology, evolution and biomechanics of a natural perturbation.
456 *Biological Journal of the Linnean Society* 124:279–293. doi:10.1093/biolinnean/bly05
- 457 Kar DC, Kurien Issac K, Jayarajan K. 2003. Gaits and energetics in terrestrial legged
458 locomotion. *Mechanism and Machine Theory* 38:355–366. doi:10.1016/S0094-
459 114X(02)00124-6
- 460 Koditschek DE, Full RJ, Buehler M. 2004. Mechanical aspects of legged locomotion control.
461 *Arthropod Structure and Development* 33:251–272. doi:10.1016/j.asd.2004.06.003.
- 462 Kram R, Wong B, Full RJ. 1997. Three-dimensional kinematics and limb kinetic energy of
463 running cockroaches. *Journal of Experimental Biology* 200:1919–29.
- 464 Mendes CS, Bartos I, Akay T, Márka S, Mann RS. 2013. Quantification of gait parameters in
465 freely walking wild type and sensory deprived *Drosophila melanogaster*. *eLife* 2013:1–24.
466 doi:10.7554/eLife.00231
- 467 Merienne H, Latil G, Moretto P, Fourcassié V 2020. Walking kinematics in the polymorphic
468 seed harvester ant *Messor barbarus*: influence of body size and load carriage. *Journal of*
469 *Experimental Biology*, 223: jeb205690. doi: 10.1242/jeb.205690
- 470 Moll K, Roces F, Federle W. 2010. Foraging grass-cutting ants (*Atta vollenweideri*) maintain
471 stability by balancing their loads with controlled head movements. *Journal of Comparative*
472 *Physiology* 196:471–480. doi:10.1007/s00359-010-0535-3
- 473 Moll K, Roces F, Federle W. 2013. How load-carrying ants avoid falling over: mechanical
474 stability during foraging in *Atta vollenweideri* grass-cutting ants. *PLoS ONE* 8:1–9.
475 doi:10.1371/journal.pone.0052816
- 476 Peters RS, Krogmann L, Mayer C, Donath A, Gunkel S, Meusemann K, Kozlov A,
477 Podsiadlowski L, Petersen M, Lanfear R, Diez PA, Heraty J, Kjer KM, Klopstein S, Meier
478 R, Polidori C, Schmitt T, Liu S, Zhou X, Wappler T, Rust J, Misof B, Niehuis O. 2017.
479 Evolutionary history of the Hymenoptera. *Current Biology*, 27: 1013-1018.
480 doi:10.1016/j.cub.2017.01.027

- 481 Pfeffer, S.E., Wahl, V.L., Wittlinger, M., Wolf, H. 2019. High-speed locomotion in the Saharan
482 silver ant, *Cataglyphis bombycina*. *Journal of Experimental Biology*, 222, jeb198705.
483 doi:10.1242/jeb.198705
- 484 Pfeffer SE, Wahl VL, Wittlinger M. 2016. How to find home backwards? Locomotion and inter-
485 leg coordination during rearward walking of *Cataglyphis fortis* desert ants. *Journal of*
486 *Experimental Biology* 219:2110–2118. doi:10.1242/jeb.137778
- 487 Polidori C, Crottini A, Venezia D, Selfa J, Saino N, Rubolini D. 2013. Food load manipulation
488 ability shapes flight morphology in females of central-place foraging Hymenoptera.
489 *Frontiers in Zoology*, 10. doi:10.1186/1742-9994-10-36
- 490 Reinhardt L, Blickhan R. 2014. Level locomotion in wood ants: evidence for grounded running.
491 *Journal of Experimental Biology* 217:2358–2370. doi:10.1016/j.j.zool.2007.01.003
- 492 Reinhardt L, Weihmann T, Blickhan R. 2009. Dynamics and kinematics of ant locomotion: do
493 wood ants climb on level surfaces? *Journal of Experimental Biology* 212:2426–2435.
494 doi:10.1242/jeb.026880
- 495 Ridgel AL, Ritzmann RE. 2005. Insights into age-related locomotor declines from studies of
496 insects. *Ageing Research Reviews* 4:23–39. doi:10.1016/j.arr.2004.08.002
- 497 Seidl T, Wehner R. 2008. Walking on inclines: how do desert ants monitor slope and step length.
498 *Frontiers in Zoology* 5:1–15. doi:10.1186/1742-9994-5-8
- 499 Spence AJ, Revzen S, Seipel J, Mullens C, Full RJ. 2010. Insects running on elastic surfaces.
500 *Journal of Experimental Biology* 213:1907–1920. doi:10.1242/jeb.042515
- 501 Uhlmann V, Ramdya P, Delgado-Gonzalo R, Benton R, Unser M. 2017. FlyLimbTracker: An
502 active contour based approach for leg segment tracking in unmarked, freely behaving
503 *Drosophila*. *PLoS ONE* 12:1–21. doi:10.1371/journal.pone.0173433
- 504 Vereecke EE, D’Août K, Aerts P. 2006. The dynamics of hylobatid bipedalism: evidence for an
505 energy-saving mechanism? *Journal of Experimental Biology* 209:2829–2838. doi:
506 10.1242/jeb.02316
- 507 Wahl V, Pfeffer SE, Wittlinger M. 2015. Walking and running in the desert ant *Cataglyphis*
508 *fortis*. *Journal of comparative Physiology A*, 201: 645-656. doi:10.1007/s00359-015-0999-2

- 509 Watson JT, Ritzmann RE, Zill SN, Pollack AJ. 2002. Control of obstacle climbing in the
510 cockroach, *Blaberus discoidalis*. I. Kinematics. *Journal of Comparative Physiology A:*
511 *Neuroethology, Sensory, Neural, and Behavioral Physiology* 188:39–53.
512 doi:10.1007/s00359-002-0277-y
- 513 Wöhrl T, Reinhardt L, Blickhan R. 2017. Propulsion in hexapod locomotion: how do desert ants
514 traverse slopes? *Journal of Experimental Biology* 220:1618–1625. doi:10.1242/jeb.137505
- 515 Wosnitza A, Bockemuhl T, Dubbert M, Scholz H, Buschges A. 2012. Inter-leg coordination in
516 the control of walking speed in *Drosophila*. *Journal of Experimental Biology* 216:480–491.
517 doi:10.1242/jeb.078139
- 518 Zolliköfer CPE. 1994. Stepping patterns in ants - Part III - Influence of load. *The Journal of*
519 *Experimental Biology* 192:119–127.
- 520

Table 1: Effect of body mass on the kinematics of unloaded ants. The results of a power law model describing the influence of ant mass M (in mg) on each variable Y , with $Y=a M^b$, are indicated on each line of the table. The first column gives the model prediction, along with its 95% confidence interval, for the mean value of ant masses (12.5 mg). The second and third column give the value of the coefficient a and b for ant mass respectively, along with their 95% confidence interval. The adjusted R^2 for the model is given in the fourth column. Bold characters indicate that 0 is not included in the 95% confidence interval of the coefficient b for ant mass. $N = 52$ ants.

Table 2: Effect of body mass and load ratio on the changes in kinematics between unloaded and loaded locomotion. The results of a power law model describing the influence of ant mass M (in mg) and load ratio LR on the relative changes of variables Y between the loaded and unloaded condition are indicated on each line of the table. The equation of the model is $Y_l/Y_u = c M^d LR^e$ with Y_u and Y_l the value of the variable in the unloaded and loaded condition, respectively. The first column gives the model prediction, along with its 95% confidence interval for the mean value of ant masses (12.5 mg) and a load ratio of 1 (unloaded ants). The second, third and fourth column give the value of the coefficients c and d for ant mass, and that of the coefficient e for load ratio, respectively, along with their 95% confidence interval. The adjusted R^2 for the model is given in the fifth column. If the value of a coefficient is positive (i.e. c , d or e) this means that the value of Y in loaded condition increases compared to unloaded condition when the explanatory variable increases and vice versa. Bold characters indicate that 0 is not included in the 95% confidence interval of the coefficient d for ant mass and e for load ratio. Because ants moved along a straight path, we averaged the values of the variables for the right and left leg of each pair of legs. $N = 52$ ants.

Figure 1: Position of the tracked points on each ant. The pictures show (A, C) a view from the top and (B, D) a view from the side of the same ant (mass = 10.1 mg) tested in (A, B) unloaded and (C, D) loaded condition (load mass = 3.5mg). The X axis in (C) stands for the longitudinal body axis while the Y axis stands for the transverse body axis. The tracked points are shown in red. The filled blue points in (D) show the positions of the overall CoM of the ant in the unloaded and loaded condition. The arrow shows the shift in the position of the overall CoM between the unloaded and loaded condition.

Figure 2: Body mass and load ratio of tested ants. The points represent small ants (blue, $N = 27$), big ants (red, $N = 27$), low load ratio (empty dots, $N = 27$) and high load ratio (filled dots, $N = 27$). The thin vertical and horizontal lines correspond to the median body mass and median load ratio, respectively.

Figure 3: Variation of the vertical position and norm of the velocity vector of the ant overall CoM. (A, C, E) mean variation of the vertical position and (B, D, F) norm of the velocity vector of the CoM. (A, B) small (blue, ant mass < 10.2 mg, $N = 27$) and big (red, ant mass > 10.2 mg, $N = 27$) for unloaded ants over one stride cycle. (C, D) small (blue, ant mass < 10.2 mg, $LR > 3$, $N = 17$) and big (red, ant mass > 10.2 mg, $LR > 3$, $N = 10$) ants loaded with high load ratio ($LR > 3$). The dashed lines represent the 95% confidence interval of the mean. For the sake of clarity, all values are centered on their mean.

Figure 4: Variation of the mechanical energies of the CoM relative to the surroundings. The mean variation of the kinetic (orange), potential (light blue) and external (black) mechanical energies over one stride cycle are shown for (A) small unloaded ants (ant mass < 10.2 mg, $N = 27$). (B) big unloaded ants (ant mass > 10.2 mg, $N = 27$). (C) small loaded ants with small load ratio (ant mass < 10.2 mg, load ratio < 3, $N = 9$). (D) big loaded ants with small load ratio (ant mass > 10.2 mg, load ratio < 3, $N = 17$). (E) small loaded ants with high load ratio (ant mass < 10.2 mg, load ratio > 3, $N = 18$). (F) big loaded ants with high load ratio (ant mass > 10.2 mg, load ratio > 3, $N = 10$). For the sake of clarity, the values of energies are centered on their mean.

Figure 5: Correlation coefficient and phase lag between the kinetic and potential energies of the CoM. (A) Correlation coefficient and (B) phase lag between the CoM E_p and E_k for unladen ants and loaded ants. The results are shown for small (blue) and big ants (red). * indicates that the difference between samples is significant according to a Welch two sample t-test ($P < 0.05$). The line within the box represents the median, the lower and upper boundaries represent respectively the 25th and 75th percentiles while the whiskers extend to the smallest and largest values within 1.5 box lengths. The notch in each bar represents the confidence interval of the median. $N = 52$ ants.

Figure 6: External mechanical work and power for unloaded ants. (A) external mechanical work ($F_{1,52} = 1502$, $P < 0.001$) and (B) external mechanical power ($F_{1,52} = 717$, $P < 0.001$). The straight line gives the prediction of a linear regression model and the dashed lines the 95% confidence interval of the slope of the regression line ($N = 52$ ants).

Table 1 (on next page)

Effect of body mass on the kinematics of unloaded ants.

Walking kinematics in the polymorphic seed harvester ant *Messor barbarus*: influence of body size and load carriage The results of a power law model describing the influence of ant mass M (in mg) on each variable Y , with $Y = a M^b$, are indicated on each line of the table. The first column gives the model prediction, along with its 95% confidence interval, for the mean value of ant masses (12.5 mg). The second and third column give the value of the coefficient a and b for ant mass respectively, along with their 95% confidence interval. The adjusted R^2 for the model is given in the fourth column. Bold characters indicate that 0 is not included in the 95% confidence interval of the coefficient b for ant mass. $N = 52$ ants.

	Variable	Model prediction for mean(ant mass) [CI]	Coefficient a [CI]	Coefficient b for ant mass [CI]	Adj R ²
1	RMSE speed norm	0.134 [0.124;0.145]	0.148 [0.119;0.184]	-0.038 [-0.129; 0.052]	0.00
2	RMSE Z position	0.143 [0.129;0.158]	0.160 [0.121;0.212]	-0.044 [-0.161; 0.073]	0.00
3	Z position amplitude (BL ¹)	0.015 [0.014;0.017]	0.048 [0.037;0.062]	-0.451 [-0.555;-0.347]	0.59
4	Mean Z position (BL)	0.121 [0.115;0.128]	0.278 [0.238;0.324]	-0.326 [-0.389;-0.262]	0.67
5	Body angle (°)	11.77 [10.85;12.76]	14.71 [11.68;18.52]	-0.088 [-0.183; 0.008]	0.04
6	Correlation coefficient	0.411 [0.355;0.475]	0.695 [0.459;1.053]	-0.206 [-0.379;-0.034]	0.09
7	Percentage congruity (%)	66.18 [64.33;68.09]	72.62 [66.97;78.74]	-0.036 [-0.070;-0.003]	0.07
8	Ek / Ep phase (°)	26.42 [21.81;32.00]	9.864 [5.637;17.26]	0.387 [0.157; 0.616]	0.18
9	Mass specific Wext (nJ/mm/mg)	1.072 [1.027;1.120]	1.050 [0.929;1.187]	0.008 [-0.043; 0.059]	0.00
10	Mass specific Pext (nJ/s/mg)	30.94 [28.58;33.49]	29.32 [23.40;36.75]	0.021 [-0.073; 0.115]	0.00
11	Percentage recovery (%)	8.200 [7.392;9.097]	6.407 [4.770;8.606]	0.097 [-0.026; 0.219]	0.03

1 ¹ BL= Body Length

Table 2 (on next page)

Effect of body mass and load ratio on the changes in kinematics between unloaded and loaded locomotion.

Walking kinematics in the polymorphic seed harvester ant *Messor barbarus*: influence of body size and load carriage The results of a power law model describing the influence of ant mass M (in mg) and load ratio LR on the relative changes of variables between the loaded and unloaded condition are indicated on each line of the table. The equation of the model is $Y_l/Y_u = c M^d LR^e$ with Y_l and Y_u the value of the variable in the unloaded and loaded condition, respectively. The first column gives the model prediction, along with its 95% confidence interval for the mean value of ant masses (12.5 mg) and a load ratio of 1 (unloaded ants). The second, third and fourth column give the value of the coefficients c and d for ant mass, and that of the coefficient e for load ratio, respectively, along with their 95% confidence interval. The adjusted R^2 for the model is given in the fifth column. If the value of a coefficient is positive (i.e. c , d or e) this means that the value of Y in loaded condition increases compared to unloaded condition when the explanatory variable increases and vice versa. Bold characters indicate that 0 is not included in the 95% confidence interval of the coefficient d for ant mass and e for load ratio. Because ants moved along a straight path, we averaged the values of the variables for the right and left leg of each pair of legs. $N = 52$ ants.

Variable (ratio loaded / unloaded)	Model prediction for mean(ant mass) and LR=1 [CI]	Coefficient c [CI]	Coefficient for d for ant mass [CI]	Coefficient for e for load ratio [CI]	Adj R ²
1 RMSE Speed norm	0.912 [0.679;1.225]	0.700 [0.413;1.187]	0.104 [-0.033; 0.241]	0.208 [-0.062; 0.478]	0.02
2 RMSE Z position	0.863 [0.615;1.212]	0.584 [0.318;1.072]	0.154 [-0.004; 0.311]	0.412 [0.101; 0.722]	0.10
3 Z position amplitude (BL ¹)	1.242 [0.836;1.845]	1.115 [0.548;2.266]	0.042 [-0.141; 0.226]	0.011 [-0.352; 0.373]	0.02
4 Mean Z position (BL)	0.917 [0.755;1.113]	0.874 [0.617;1.238]	0.019 [-0.071; 0.109]	-0.062 [-0.240; 0.116]	0.01
5 Body angle (°)	0.884 [0.440;1.774]	0.645 [0.175;2.378]	0.120 [-0.226; 0.467]	-0.622 [-1.274; 0.030]	0.09
6 Correlation coefficient	1.353 [0.835;2.194]	0.996 [0.419;2.366]	0.121 [-0.104; 0.345]	-0.212 [-0.654; 0.230]	0.04
7 Percentage congruity (%)	1.116 [1.012;1.231]	1.186 [0.995;1.414]	-0.024 [-0.069; 0.022]	-0.176 [-0.266;-0.086]	0.22
8 Ek / Ep phase (°)	2.174 [0.766;6.171]	12.07 [1.816;80.30]	-0.663 [-1.183;-0.143]	-0.995 [-1.988;-0.001]	0.14
9 Mass specific Wext (nJ/mm/mg)	1.120 [0.917;1.367]	0.852 [0.596;1.218]	0.107 [0.015; 0.200]	0.454 [0.271; 0.636]	0.31
10 Mas specific Pext (nJ/s/mg)	1.202 [0.862;1.676]	1.153 [0.636;2.091]	0.016 [-0.138; 0.171]	-0.255 [-0.559;0.049]	0.04
11 Percentage recovery (%)	0.883 [0.571;1.367]	1.090 [0.498;2.384]	-0.082 [-0.285;0.120]	-0.144 [-0.544;0.255]	0.01

1 ¹ BL= Body Length

2

Figure 1

Position of the tracked points on each ant.

The pictures show (A, C) a view from the top and (B, D) a view from the side of the same ant (mass = 10.1 mg) tested in (A, B) unloaded and (C, D) loaded condition (load mass = 3.5mg). The X axis in (C) stands for the longitudinal body axis while the Y axis stands for the transverse body axis. The tracked points are shown in red. The filled blue points in (D) show the positions of the overall CoM of the ant in the unloaded and loaded condition. The arrow shows the shift in the position of the overall CoM between the unloaded and loaded condition

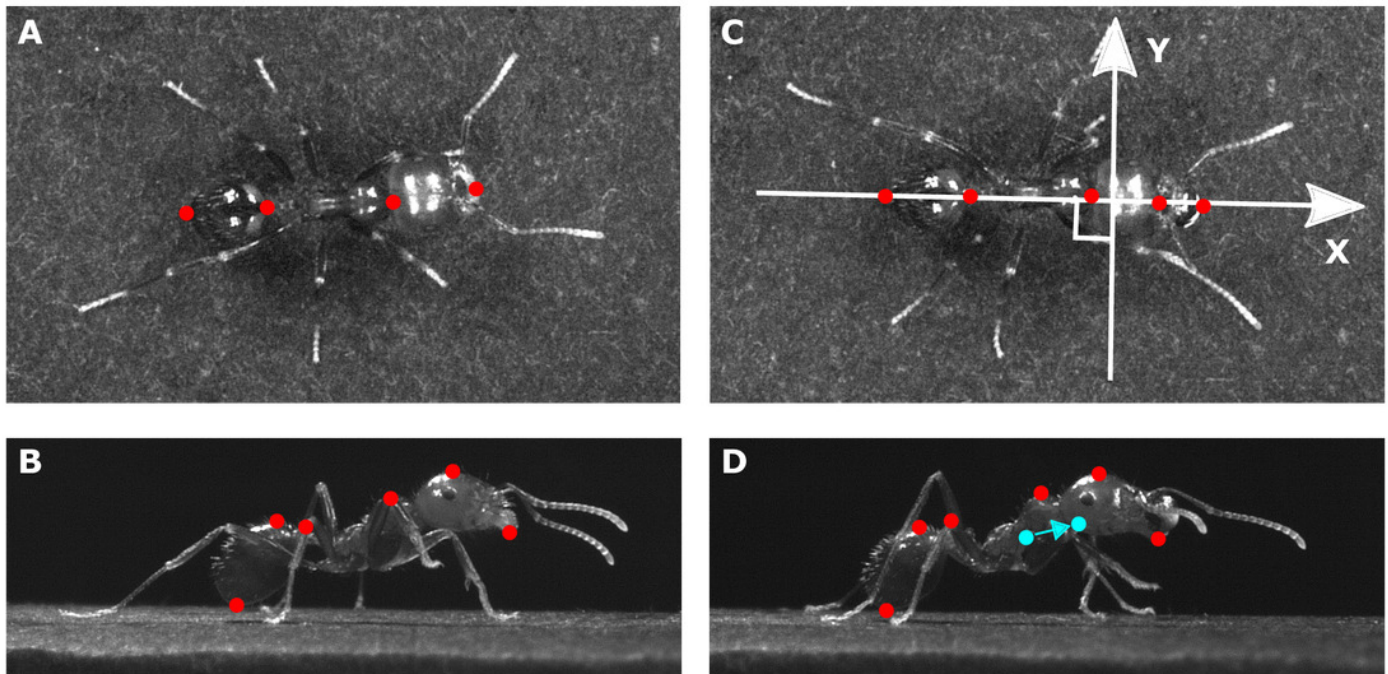


Figure 2

Body mass and load ratio of tested ants.

The points represent small ants (blue, $N = 27$), big ants (red, $N = 27$), low load ratio (empty dots, $N = 27$) and high load ratio (filled dots, $N = 27$). The thin vertical and horizontal lines correspond to the median body mass and median load ratio, respectively.

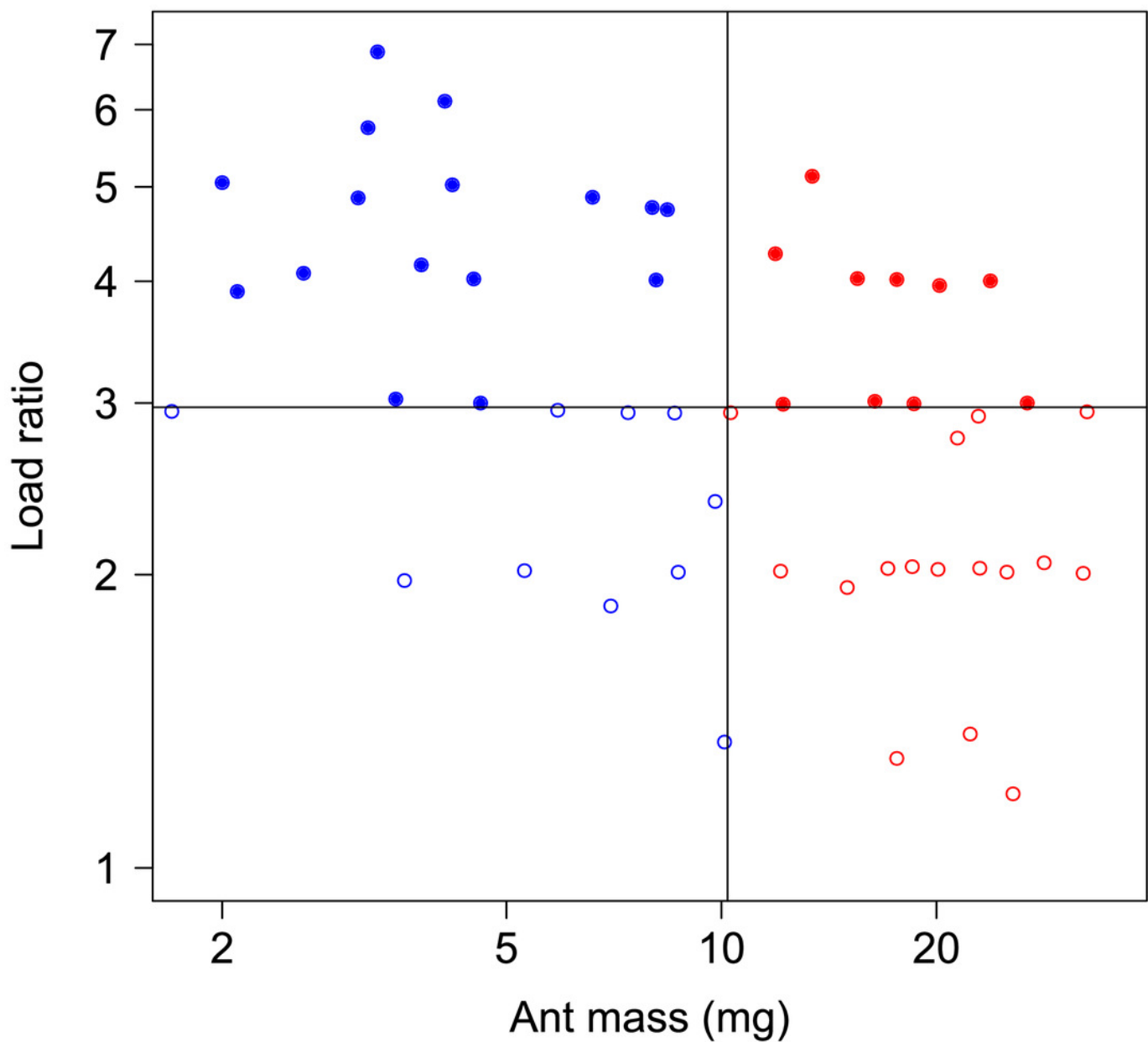


Figure 3

Variation of the vertical position and norm of the velocity vector of the ant overall CoM.

(A, C, E) mean variation of the vertical position and (B, D, F) norm of the velocity vector of the CoM. (A, B) small (blue, ant mass < 10.2 mg, N = 27) and big (red, ant mass > 10.2 mg, N = 27) for unloaded ants over one stride cycle. (C, D) small (blue, ant mass < 10.2 mg, LR > 3, N = 17) and big (red, ant mass > 10.2 mg, LR > 3, N = 10) ants loaded with high load ratio (LR>3). The dashed lines represent the 95% confidence interval of the mean. For the sake of clarity, all values are centered on their mean

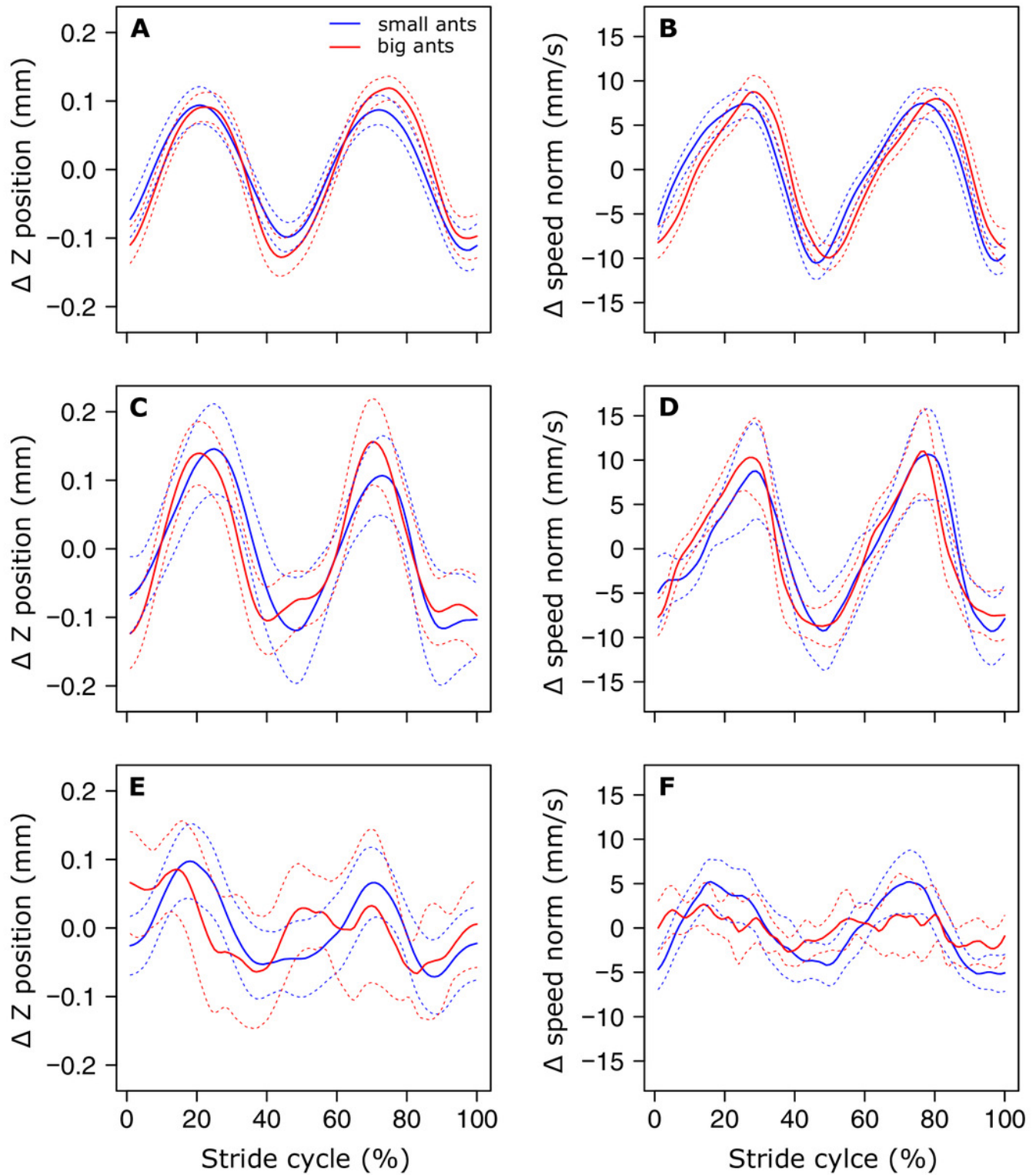


Figure 4

Variation of the mechanical energies of the CoM relative to the surroundings.

The mean variation of the kinetic (orange), potential (light blue) and external (black) mechanical energies over one stride cycle are shown for (A) small unloaded ants (ant mass < 10.2 mg, N = 27). (B) big unloaded ants (ant mass > 10.2 mg, N = 27). (C) small loaded ants with small load ratio (ant mass < 10.2 mg, load ratio < 3, N = 9). (D) big loaded ants with small load ratio (ant mass > 10.2 mg, load ratio < 3, N = 17). (E) small loaded ants with high load ratio (ant mass < 10.2 mg, load ratio > 3, N = 18). (F) big loaded ants with high load ratio (ant mass > 10.2 mg, load ratio > 3, N = 10). For the sake of clarity, the values of energies are centered on their mean.

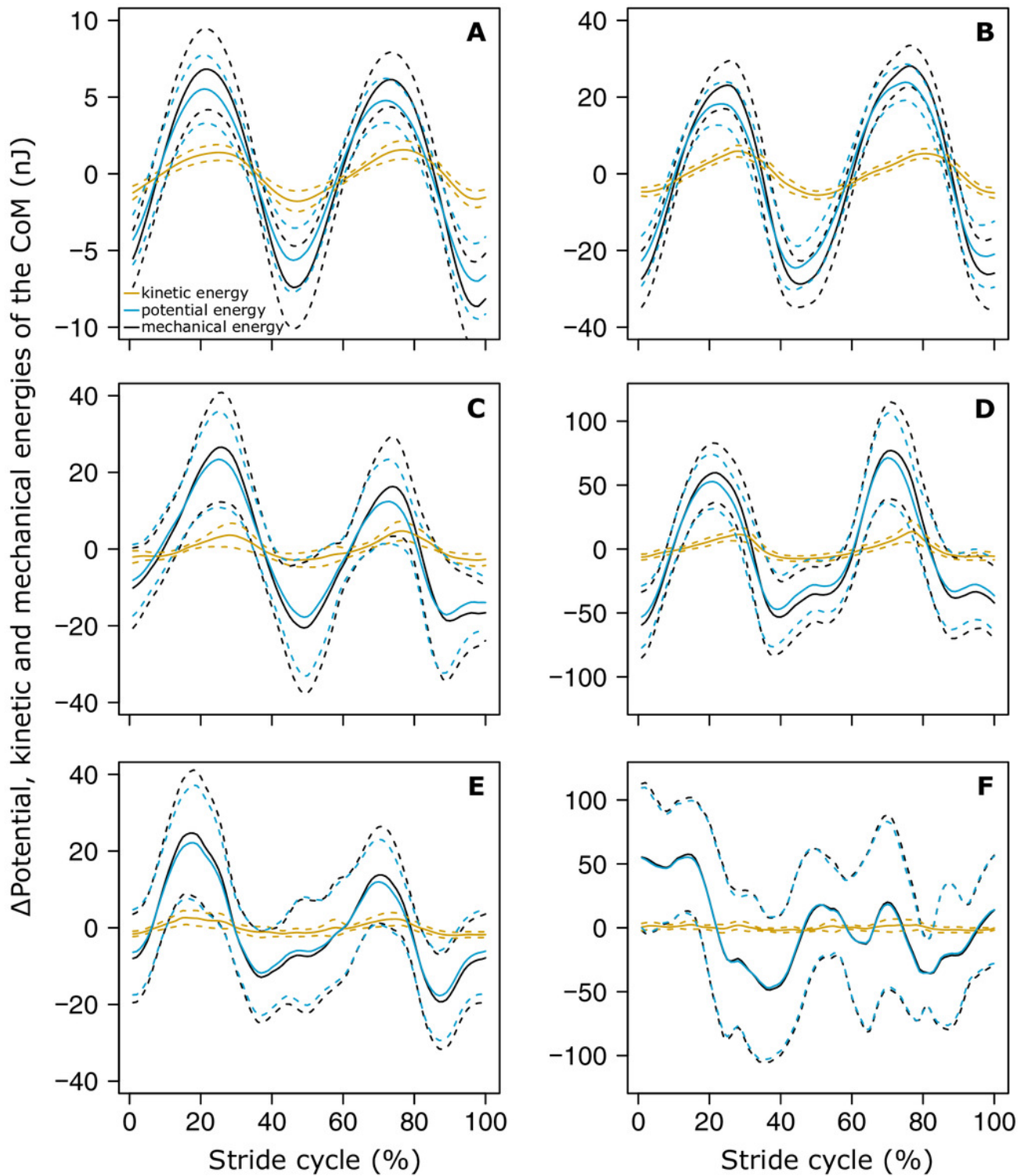


Figure 5

Correlation coefficient and phase lag between the kinetic and potential energies of the CoM.

(A) Correlation coefficient and (B) phase lag between the CoM E_p and E_k for unladen ants and loaded ants. The results are shown for small (blue) and big ants (red). * indicates that the difference between samples is significant according to a Welch two sample t-test ($P < 0.05$). The line within the box represents the median, the lower and upper boundaries represent respectively the 25th and 75th percentiles while the whiskers extend to the smallest and largest values within 1.5 box lengths. The notch in each bar represents the confidence interval of the median. $N = 52$ ants.

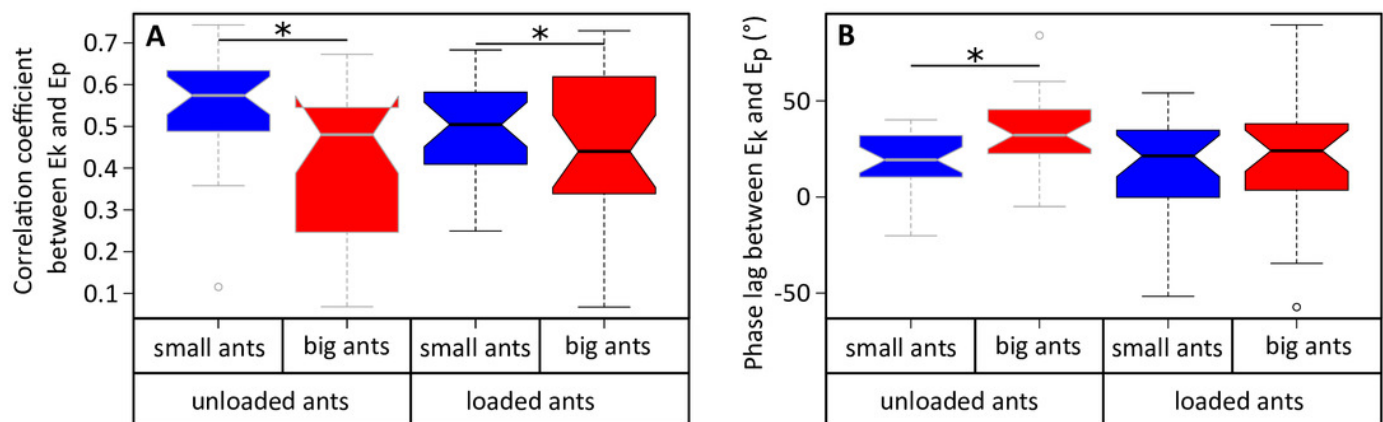


Figure 6

External mechanical work and power for unloaded ants.

(A) external mechanical work ($F_{1,52}=1502$, $P<0.001$) and (B) external mechanical power ($F_{1,52}=717$, $P<0.001$). The straight line gives the prediction of a linear regression model and the dashed lines the 95% confidence interval of the slope of the regression line (N= 52 ants).

